Journal of Organometallic Chemistry xxx (2017) 1–8

Contents lists available at ScienceDirect

Journal of Organometallic Chemistry

journal homepage: www.elsevier.com/locate/jorganchem

Mechanistic insights into catalytic carboxylic ester hydrogenation with cooperative Ru(II)-bis{1,2,3-triazolylidene}pyridine pincer complexes

Soraya N. Sluijter, Ties J. Korstanje, Jarl Ivar van der Vlugt*, Cornelis J. Elsevier**

van 't Hoff Institute for Molecular Sciences, University of Amsterdam, Science Park 904, 1098 XH, Amsterdam, The Netherlands

ARTICLE INFO

Article history:
Received 10 November 2016
Received in revised form
5 January 2017
Accepted 6 January 2017
Available online xxx

Keywords:
Pincer ligand
Ruthenium
Carboxylic ester
Hydrogenation
Catalysis

ABSTRACT

Transmetallation of newly designed lutidine-based CNC or CNN ligands **L**, featuring flanking 1,2,3-triazolylidene (tzNHCs) moieties, from Ag(I) to Ru(II) provided access to well-defined cationic $[Ru^{II}(CO)(H)(\mathbf{L})(PPh_3)]^+$ complexes **2** and **5**. Spectroscopic investigations confirm that, in both complexes, the tridentate ligand binds in a rare facial mode to the metal center. The complexes, that exhibit ligand-based reversible deprotonation/dearomatization reactivity, are active in catalytic ester hydrogenation in the presence of KO*t*Bu (≥20 mol%) as an exogenous base. The beneficial effect of the base on catalytic activity relates to transesterification of substrates to the corresponding *tert*-butyl ester derivatives, which are hydrogenated considerably faster than methyl esters. The mechanistic findings in this work confirm that this transformation is very complex, with this transesterification, metal-ligand cooperative reactivity, base strength and possibly product inhibition all playing a role. Furthermore, relevant Ru(CNC)(hydride) species have been observed by NMR spectroscopy under near-catalytic conditions.

1. Introduction

The design of rigid tridentate ligands with a preference for a meridional coordination mode, commonly referred to as 'pincer' ligands, is still drawing much attention, nearly four decades after the initial reports on their coordination chemistry [1]. The original 'design' of a monoanionic alkyl- or arene-based carbon donor with two flanking heteroatom donors ('ECE') has been significantly expanded, not only with respect to the 'core' donor, but also the overall charge of the ligand in coordination complexes and the rigidity of the overall framework. Amidst the plethora of pincer ligand designs that have been developed, platforms that allow for active ligand participation in bond activation and functionalization processes have emerged in the last decade. These 'reactive' ligand classes often operate via some type of internal basic moiety that can undergo reversible proton-transfer. This may involve reversible alcohol-alcoholate [2], secondary amine-amide [3], sulfonaminephosphine-sulfonamidophosphine [4] or pyrazole-pyrazolate [5] switching. Also reversible cyclometalation has been reported as concept for cooperative bond activation [6]. Reversible dearomatization of heteroatom donor sidearm functionalized picoline or lutidine designs has emerged as 'privileged' concept for the (intramolecular) dehydrogenative coupling as well as hydrogenation of a wide variety of substrates [7]. Typically, these scaffolds are decorated with phosphines or amines, whereas N-heterocyclic carbene side-groups have been relatively underexplored to date.

Carboxylic ester hydrogenation (Scheme 1) is an industrially important transformation to produce alcohols [8]. Biomass feedstocks, such as vegetable fats and oils, contain many ester functionalities. Considering the depletion of fossil fuels, ester hydrogenation may therefore play a pivotal role in the transition to a biobased chemical industry. Currently, non-selective heterogeneous catalysts (typically based on copper chromite) that require high pressures and temperatures are used to perform this reaction [9]. Homogeneous catalysts may allow both better chemoselectivity and milder reaction conditions. Early reports on ruthenium-based catalysts for the hydrogenation of esters required additives, harsh conditions and/or were only suitable for activated esters [10].

The hydrogenation of carboxylic esters to alcohols, formally called hydrogenolysis, is far more difficult compared to ketone

* Corresponding author.
** Corresponding author.
E-mail addresses: j.i.vandervlugt@uva.nl (J.I. van der Vlugt), c.j.elsevier@uva.nl (C.J. Elsevier).

http://dx.doi.org/10.1016/j.jorganchem.2017.01.003
0022-328X/

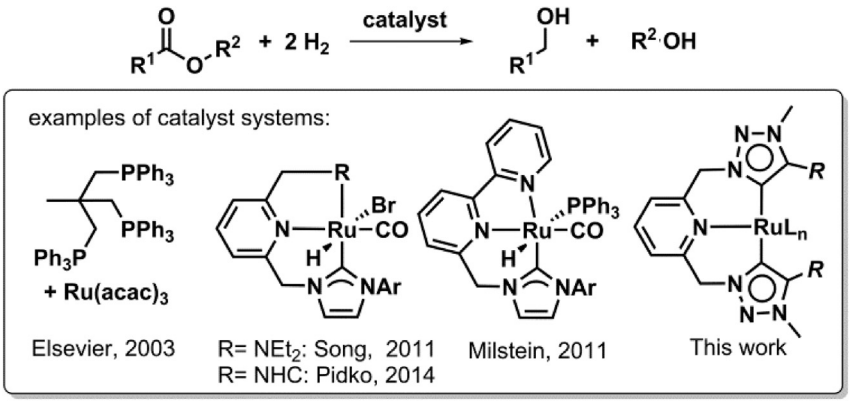

Scheme 1. Generic reaction for ester hydrogenation (top), a selection of Ru pre-catalysts for this reaction and the generic structure of the target complexes disclosed herein (bottom).

hydrogenation because the ester C═O double bond is a weak electrophile that is stabilized by resonance. Our group was among the first to convert esters to alcohols at reasonable temperature and pressure (100 °C and 70 bar) using a homogeneous ruthenium(-triphos) catalyst (triphos = 1,1,1-tris(diphenylphosphinomethyl) ethane; Scheme 1) [11]. In the last decade, significant progress in ester hydrogenolysis catalyzed by well-defined transition metal complexes based on lutidine-derived pincer ligands has been achieved (Scheme 1) [12]. In several cases, the reactivity can be attributed to the existence of accessible metal-ligand cooperative (MLC) pathways [13].

Ester hydrogenation mechanisms are still under debate and have thus far not been proven unequivocally [14]. A plausible proposed catalytic cycle for ester hydrogenation catalyzed by a cooperative Ru(hydride) complex is depicted in Scheme 2. The rate limiting step of this reaction has generally been considered to be hydrogen transfer to the stabilized ester carbonyl moiety to generate a hemiacetal (Scheme 2, I). On the basis of DFT calculations three mechanisms have been proposed for this step: a) carbonyl insertion (via a 4-membered ring Ru-O-C-H transition state) [15], b) H/OR metathesis [16] and c) ligand assisted hydride transfer [17]. In order to facilitate the hydrogen transfer, electron-rich ligands can be employed to enhance the nucleophilicity of the hydride towards the substrate. This is nicely illustrated by the rate enhancement upon replacing a phosphine donor for a more electron-donating NHC moiety [18]. The ligand can also play a role in hemiacetal decomposition (Scheme 2, III), by promoting C-O bond cleavage of the intermediate, which might lead to the alternatively proposed Ru(alkoxide) species [19]. The cooperative reactivity of deprotonated *N*-heterocyclic carbene-based CNC ligands is more pronounced compared to phosphine-containing PNP systems, which has been attributed to a combination of electronic properties and extended flexibility of the larger CNC chelate [20]. Alternatively, an outer-sphere bifunctional mechanism has been suggested to be operational for these systems [21].

In this contribution, the synthesis and catalytic application of novel CNC and CNN pincer ligands bearing flanking 1,2,3-triazolylidene (tzNHC) [22] moieties and a central pyridine donor are described. The corresponding Ru^{II} complexes have been applied in catalytic ester hydrogenolysis. Considering the correlation

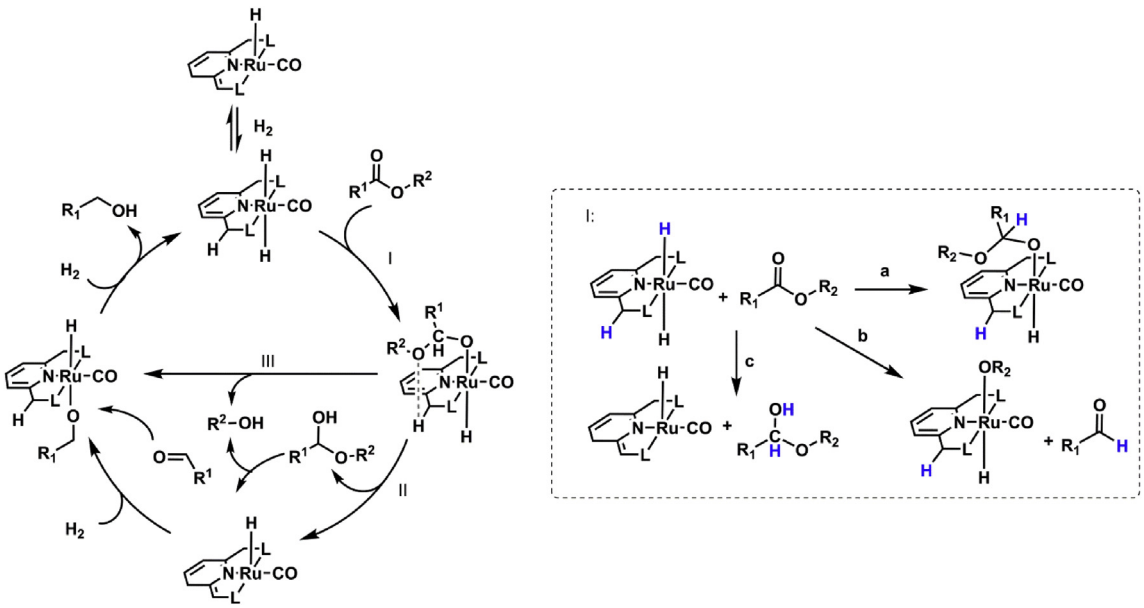

Scheme 2. Proposed catalytic cycle for the Ru-catalyzed hydrogenation of carboxylic esters to alcohols using metal-ligand cooperative systems. Box: proposed mechanisms for hydrogen transfer (I): a) carbonyl insertion, b) H/OR metathesis and c) ligand assisted hydride transfer.

Please cite this article in press as: S.N. Sluijter, et al., Journal of Organometallic Chemistry (2017), http://dx.doi.org/10.1016/j.jorganchem.2017.01.003

between electron density and catalytic ester hydrogenation activity, it is hypothesized that the strong tzNHC donors in these ligands may enhance the hydricity of a Ru(hydride) fragment, leading to higher catalyst activity. Furthermore, we have investigated the mechanistic aspects of the ester hydrogenation such as the role of the base, additives, MLC reactivity and the nature of potentially relevant species in the catalytic reaction.

2. Results and discussion

2.1. Synthesis of the CNC and CNN ligands

The desired CNC ligand **L1** was efficiently synthesized in two steps from commercially available starting materials (Scheme 3) [23]. To the best of our knowledge, only one tridentate (pincer) ligand bearing two triazolylidene moieties is known [24] and **L1** is the first to be tested in catalysis. We were also interested to obtain the CNN analogue **L2**, because the potential hemilability of the triazole moiety might have a positive effect on the catalytic ester hydrogenolysis. When only one equivalent of methylating agent was reacted with intermediate **A**, a mixture of starting material, mono- and bis(methylated) product was obtained. The three different species were easily separated by column chromatography, providing access to the CNN pincer ligand **L2** (Scheme 3).

2.2. Synthesis of Ru(II) complexes

Silver(I) complex **1** was obtained by stirring the CNC ligand **L1** in the presence of Ag_2O in MeOH for two days (Scheme 4) [25]. The formation of the desired complex was confirmed by the disappearance of the triazolium hydrogen signal in the ^1H NMR spectrum. The high resolution mass spectrum (HR-MS) corresponds to a 1:1 ratio of the silver and ligand, which suggests the presence of mononuclear structure $[Ag\mathbf{L1}]^+$ with the two tzNHC groups coordinating to the silver center in a linear fashion [26]. Unlike what was reported for Ru-complexes with bis(NHC)pyridine systems [27], direct deprotonation of the triazolium fragments of **L1** using various bases in the presence of various ruthenium precursors was unsuccessful. However, silver complex **1** proved to be a useful reagent for transmetalation to generate *fac*-$[Ru(CO)(H)(\mathbf{L1})(PPh_3)]BF_4$ (complex **2**; *fac* = facial) by reaction of **1** and $[RuCl(CO)(H)(PPh_3)_3]$ in THF at 55 °C for 2 days (Scheme 4). The surprising *fac*-coordination mode of ligand **L1** to the ruthenium center was deduced from the combined ^1H, $^{31}P\{^1H\}$ and $^{13}C\{^1H\}$ NMR spectroscopic data [28]. As a consequence of the inherent nonsymmetrical character of the ligand binding, separate signals for each hydrogen and carbon atom are observed by ^1H and $^{13}C\{^1H\}$ NMR spectroscopy. Most indicative are the distinctive signals for both triazolylidene carbons at δ 172.2 ($^2J_{CP}$ = 7.2 Hz, *cis* to PPh_3) and 164.9 ppm ($^2J_{CP}$ = 75.7 Hz, *trans* to PPh_3) in the $^{13}C\{^1H\}$ NMR spectrum. The hydrido and PPh_3 ligands were observed as a doublet at δ −7.04 ppm ($^2J_{PH}$ = 28.9 Hz) in the ^1H NMR and a singlet at 46.7 ppm in the $^{31}P\{^1H\}$ NMR spectrum, respectively. These data are consistent with the only previous report of a *fac*-Ru(CNC) complex [21]. Meridional coordination of ligand **L1** was observed in Pd(II) complex **3** (see SI), which is also accessible *via* transmetalation of Ag^I complex **1** with $[Pd(PhCN)_2Cl_2]$ [29].

For the corresponding Ag-complex **4** of CNN-ligand **L2** (Scheme 5), cold-spray ionization (CSI-)HR-MS indicated the presence of the $[Ag(CNN)_2]^+$ ion, suggesting that two ligands are coordinated to one silver center. Coordination is presumably only occurring via the triazolylidene donors, with the triazole groups remaining uncoordinated. Transmetalation to ruthenium using $[RuCl(CO)(H)(PPh_3)_3]$ generated *fac*-$[Ru(CO)(H)(\mathbf{L2})(PPh_3)]BF_4$ **5**, with the facial coordination supported by NMR spectral features. Compared to complex **2**, the hydrido and PPh_3 ligand appeared as lower frequency signals at δ −13.0 ppm ($^2J_{PH}$ = 28 Hz, *cis* to PPh_3) in the ^1H NMR and δ 40.9 ppm in the $^{31}P\{^1H\}$ NMR spectrum, respectively. In the ^{13}C NMR spectrum, the large coupling of the tzNHC carbon (166.0 ppm; $^2J_{CP}$ = 76.9 Hz) with the phosphorus atom indicates that the strongly donating NHC is located *trans* to the PPh_3 ligand. This leaves the position of the weak-field triazole-nitrogen coordinating *trans* to the hydride.

Both Ru complexes are susceptible to ligand-centered dearomatization upon reaction with one equivalent of KO*t*Bu, marked by a characteristic color change from brown-yellow to dark red. In the corresponding NMR spectrum of **2′** an upfield shift of the pyridine hydrogens and the appearance of the vinylic proton (5.52 ppm) is observed compared to **2**. The dearomatization is fully reversible, as addition of hydrochloric acid (1 M in dioxane) led to rearomatization of the pyridine ring. This chemoresponsive behaviour of the bis-triazolylidene and triazolylidene-triazole systems may be relevant for metal-ligand bifunctional ester hydrogenolysis reactivity. Furthermore, the remarkable facial

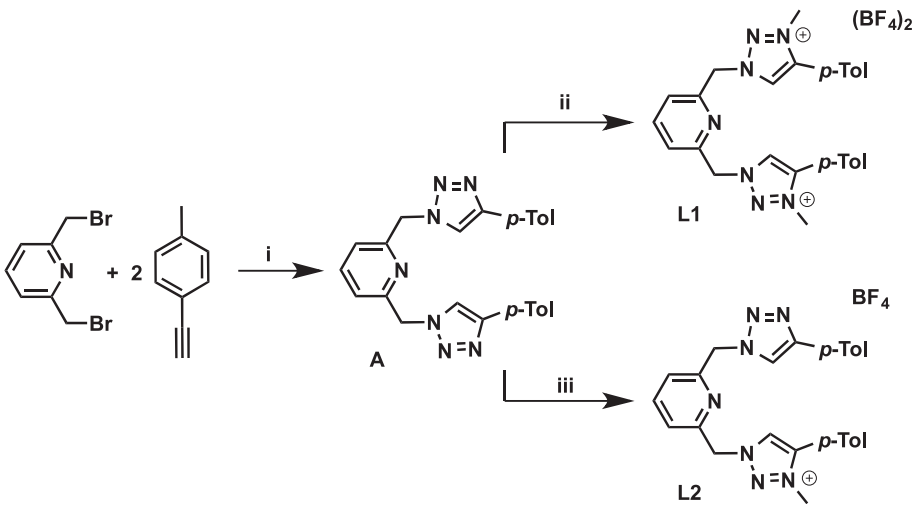

Scheme 3. Synthesis of CNC and CNN ligands **L1** and **L2**. i) NaN_3, Na_2CO_3, $CuSO_45H_2O$, sodium ascorbate, DMF/H_2O (4:1), ii) two equiv. $Me_3O\cdot BF_4$, iii) one equiv. $Me_3O\cdot BF_4$, followed by separation using column chromatography.

Please cite this article in press as: S.N. Sluijter, et al., Journal of Organometallic Chemistry (2017), http://dx.doi.org/10.1016/j.jorganchem.2017.01.003

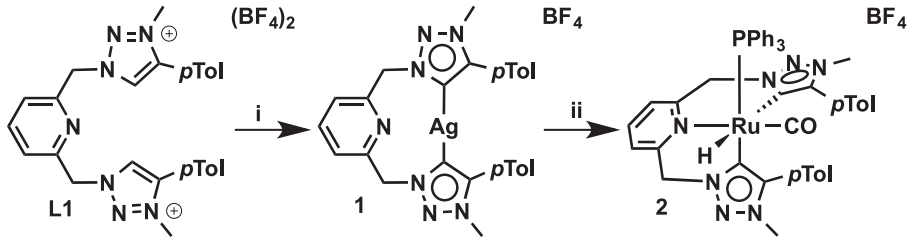

Scheme 4. Synthesis of Ag(I) complex **1** and Ru(II) complex **2**. i) Ag_2O, MeOH, 48 h; ii) $[Ru(CO)HCl(PPh_3)_3]$, THF, 55 °C, 48 h.

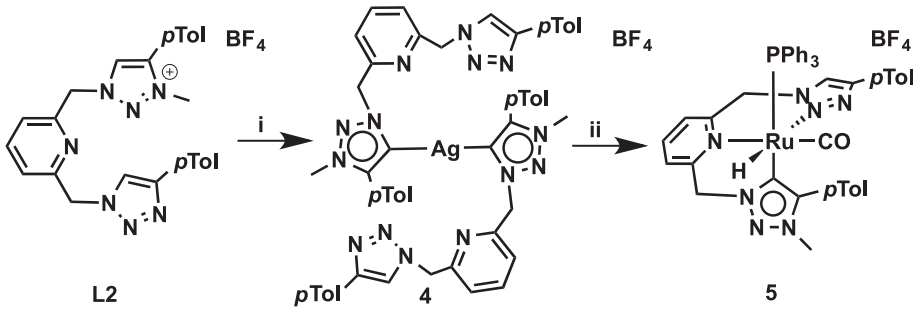

Scheme 5. Synthesis of Ru(II)(CNN) complex **5** *via* Ag(I) complex **4**. i) Ag_2O, MeOH, 48 h; ii) $[Ru(CO)HCl(PPh_3)_3]$, THF, 55 °C, 48 h.

coordination mode of these novel tridentate ligands is reminiscent of the coordination mode of the bis(thioether)amine SNS ligand in a Ru catalyst for ester hydrogenation [30].

2.3. Ruthenium catalyzed hydrogenolysis of esters

The application of **2** in the catalytic hydrogenolysis of esters was initially studied using methyl benzoate as the substrate, following the protocol described by Beller and co-workers [31]. When applying 20 mol% of KO*t*Bu, full conversion was observed within 2 h at 100 °C under 50 bar of H_2 pressure in 1,4-dioxane, using a catalyst loading of 0.75 mol% (Table 1, entry 1) [32]. At lower pressure (5 bar) the substrate was still converted, albeit at a significantly slower rate (77% conversion in 18 h). Other esters could also be hydrogenated using this system (Table 1). The aliphatic *n*-butyl benzoate was smoothly hydrogenated by complex **2** under the same reaction conditions (entry 2). Longer alkyl chains did not pose a problem either, as methyl stearate was nearly completely reduced to octadecanol within 2 h (entry 3). Methyl oleate, which contains both a carbon-carbon double bond and ester functionality, was considered an ideal substrate to test the chemoselectivity of the system (entry 4). Almost full conversion of the unsaturated fatty carboxylic ester was observed with formation of both the saturated and unsaturated product in a 2.6: 1 ratio. Following the reaction over time clearly indicated that ester hydrogenolysis is kinetically favored over C=C bond hydrogenation. The triglyceride triolein (not shown) was also converted, but several (partly unidentified) products, including octadecanol (~5%) and oleyl alcohol (~4%), were detected by GC analysis.

Hydrogenation of γ-valerolactone led to a moderate yield of 1,4-pentanediol (entry 5). Not surprisingly, given the basic reaction conditions, carboxylic acids were incompatible with the system (entries 6 and 7). Even the activated trifluoroacetic acid (TFA) was not converted at all. As expected the methyl trifluoroacetate was completely converted to trifluoroethanol (entry 8). When phenyl benzoate (entry 9) was used as substrate, only some transesterification products (*tert*-butyl benzoate and benzyl benzoate) but no benzyl alcohol were detected by GC analysis. This might be explained by the acidity of the formed phenol, neutralizing the required base [33]. Gratifyingly, the sterically hindered *tert*-butyl benzoate was hydrogenated to benzyl alcohol within 2 h (entry 10). In fact, the activity of **2** for this substrate is *higher* than for methyl benzoate (*vide infra*, Table 2).

For complex **5**, dissociation of the speculated hemilabile triazole donor in the CNN motif could result in a vacant site on the Ru center. Table 2 contains the results of methyl and *tert*-butyl benzoate hydrogenation using complex **5** *vs.* complex **2**. As no significantly improved activity of pre-catalyst **5** compared to **2** was found, we conclude that either the triazole donor is more strongly bound than anticipated (hence not displaying hemilability) or this feature does not play a critical role in the rate determining step of this catalytic reaction [34].

2.4. The role of KOtBu in the hydrogenolysis of esters

Catalyst **2** shows good activity in the hydrogenolysis of aromatic esters, but only when a minimum amount of 20 mol% of KO*t*Bu is used (Table 3, entry 1 *vs.* 2). This base dependence is also apparent for aliphatic esters (93% conversion of methyl butyrate to *n*-butanol using 20 mol% KOtBu *vs* 4% conversion using 10 mol%). The remarkable activity of complex **2** for *tert*-butyl benzoate led us to investigate whether transesterification of the ester substrates, induced by KO*t*Bu, to generate *tert*-butyl benzoate could play a role in the mechanism. Stirring methyl benzoate with 20 mol% of KO*t*Bu at 100 °C (without catalyst) led to formation of 8% *tert*-butyl benzoate, whereas with 10 mol% of base only traces (~1%) were observed. Thus, transesterification followed by hydrogenation of *tert*-butyl benzoate could be a plausible explanation for the need for 20 mol% of KO*t*Bu. From Table 3 it becomes apparent that the hydrogenation of *tert*-butyl benzoate reaches significantly higher conversion in the same reaction time than the corresponding methyl ester (entry 1 *vs* 3). Furthermore, methyl benzoate was not converted when KHMDS was applied as base, whereas the *tert*-butyl analogue was fully consumed (entry 5 *vs.* 6) [32]. This might be explained by *tert*-butoxide being a better leaving group than methoxide or by a previously observed inhibiting effect of

Please cite this article in press as: S.N. Sluijter, et al., Journal of Organometallic Chemistry (2017), http://dx.doi.org/10.1016/j.jorganchem.2017.01.003

Table 1
Substrate scope for hydrogenation catalyzed by complex **2**.

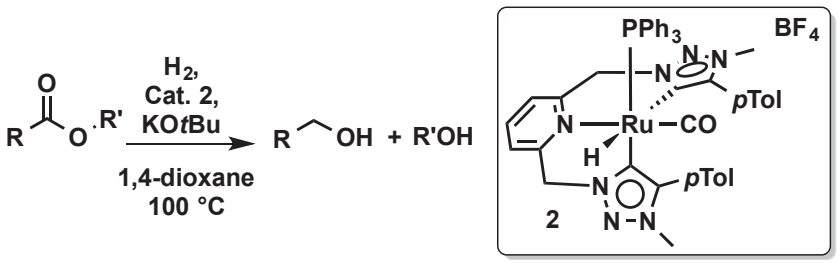

Entry	Substrate	Conv. (%)[a]	Product	Yield (%)[a]
1		53		53
2		93		93
3		93		93
4	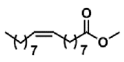	98	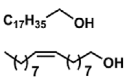	71 27
5		54	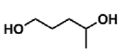	54
6		0		–
7		0		–
8		100		100
9	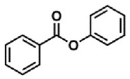	17		0
10	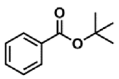	100		100

Conditions: 0.5 mmol ester substrate, 0.75 mol% of **2**, 20 mol% of KO*t*Bu, 50 bar of H_2 in 1,4-dioxane, 100 °C, 2 h.
[a] Yields were determined by GC analysis with *p*-xylene as internal standard (entries 1–6, 9 and 10) or by ^{19}F NMR spectroscopy using 1,3-bis(trifluoromethane)benzene as internal standard (entries 7 and 8).

methanol [19]. Unfortunately, decreasing the amount of base for the substrate *tert*-butyl benzoate also resulted in a large drop in conversion (entry 4). Thus, although transesterification seems to play a role in the hydrogenation of esters with **2**, it does not fully explain the need for the critical amount of base.

2.5. NMR investigations of complex 2 under near-catalytic conditions

To gain more insight in the catalytically active species, ^{1}H NMR investigations were performed. A solution of complex **2** in THF-d_8 was studied under near-catalytic conditions (20 equiv. of KO*t*Bu, 5 bar of H_2) in a J. Young pressure tube. At room temperature, the dearomatized complex **2′** was present in solution, as deduced by ^{1}H NMR spectroscopy. After the reaction mixture was heated at 100 °C for 2 h, several products were detected by NMR spectroscopy at room temperature. In the ^{31}P{^{1}H} NMR spectrum four signals were visible at 59.6, 22.9, 14.9 and −5.5 ppm, the latter being characteristic for free PPh_3. The hydride region of the ^{1}H NMR spectrum is depicted in Fig. 1 and suggests the presence of three hydride-containing Ru complexes (**2'a, 2b and 2'c** in a ~1:1:1 ratio).

Proton-coupled ^{31}P NMR spectroscopy revealed that the doublet at −6.90 ppm in the ^{1}H NMR spectrum, with a large J_{PH} coupling constant of 122 Hz, correlates with the resonance at 23 ppm in the ^{31}P{^{1}H} NMR spectrum. This *J* value indicates a mutual *trans* arrangement of the hydride and PPh_3, similar to the values reported for a related *mer*-[Ru(CNN)(CO)(H)(PPh_3)] complex [19]. Hence, the CNC ligand likely coordinates in a meridional fashion, which leads to the proposed structure of **2'a** in Fig. 1. Most likely, the ligand backbone is deprotonated in this complex, considering the large amount of base present in the mixture. Apparently, *fac-mer* isomerization of the flexible CNC chelate is possible under these conditions, for instance *via* a five-coordinated Ru species. Attempts to induce this isomerization thermally in absence of base were

Please cite this article in press as: S.N. Sluijter, et al., Journal of Organometallic Chemistry (2017), http://dx.doi.org/10.1016/j.jorganchem.2017.01.003

Table 2
Catalytic hydrogenation of methyl *vs.* *tert*-butyl benzoate with complexes **2** and **5**.

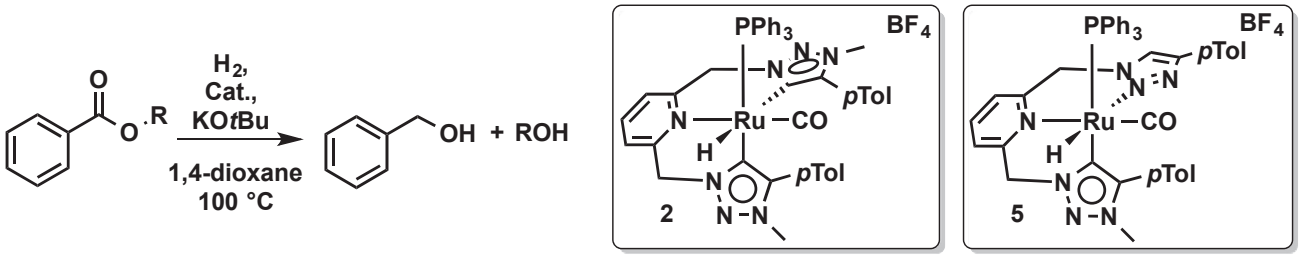

Entry	R	Cat	Yield (%)
1	Me	**2**	53
2	Me	**5**	50
3	*t*Bu	**2**	99
4	*t*Bu	**5**	100

Conditions: 0.5 mmol ester, 0.75 mol% of catalyst, 20 mol% of KO*t*Bu, 50 bar H_2 in 1,4-dioxane at 100 °C for 2 h. The yield was determined by GC analysis with *p*-xylene as internal standard.

unsuccessful.

^{1}H-^{1}H COSY combined with ^{1}H{^{31}P} NMR spectroscopy indicated that the hydride signals at −11.77 and −15.09 ppm (d, $^2J_{HH}$ = 8.4 Hz) belong to a *cis* Ru(dihydride) bearing no phosphine ligand (**2b** in Fig. 1). Considering the diamagnetic nature of this complex and the prevalence of (active) Ru(II) species, we assume that **2b** contains the protonated ligand. The remaining two signals in the hydride region at −7.53 (integrating to 1 H) and between −8.67 and −9.11 ppm (integrating to 2 H's) relate to a signal at 59.6 ppm in the ^{31}P{^{1}H} NMR spectrum. Based on integration and ^{1}H-^{1}H COSY, ^{1}H({^{31}P}) and ^{31}P({^{1}H}) spectra, T_1 measurements ($T_1 \gg$ 300 ms) and the observed patterns, which are indicative of an *ABMX* spin system, this species presumably concerns the trihydride species **2'c** that contains a deprotonated CNC-ligand but no CO ligand (Fig. 1). However, based on these data we cannot deduce which ligand arm is deprotonated.

Once the H_2 pressure was released, the mixture of species converted to the *mer*- and *fac*-ruthenium complexes **2'a** and **2′** in a ratio of approximately 2:1, which suggests that either **2b** or **2'c** contain a *mer*-coordinated CNC ligand, assuming that no *fac-mer* isomerization occurs at room temperature. However, the exact stereochemistry around the metal centers of **2b** and **2'c** has not been verified. When applying H_2 pressure and 10 equivalents of KO*t*Bu to **2** the same species **2'a-c** were observed in solution, albeit in a slightly different ratio (**2'a**: **2b**: **2'c** = 1.5: 2: 1). These NMR experiments provide initial insight in the structure of the catalytically relevant species during the hydrogenation of esters. These experiments also suggest that installment of a hemilabile donor on the ligand is not required, as the phosphine (or carbonyl group) can dissociate under (near-)catalytic conditions. Additionally, the *mer*-isomer **2′** appears to be thermally accessible.

2.6. Mechanistic considerations

The mechanistic implications of the experiments described above, including aspects related to i) metal-ligand cooperativity, ii)

Table 3
Catalytic hydrogenation of methyl *vs.* *tert*-butyl benzoate with complex **2**.

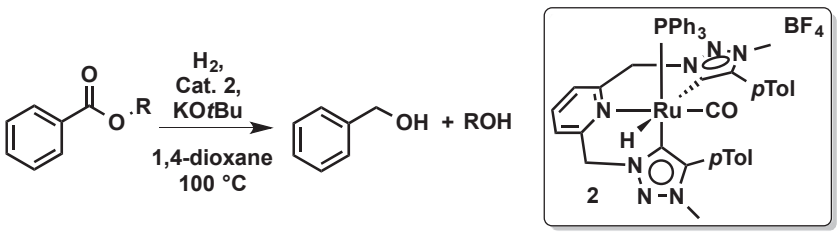

Entry	R	Base	Yield (%)
1	Me	KO*t*Bu	53
2	Me	KO*t*Bu (10 mol%)	2[a]
3	*t*Bu	KO*t*Bu	99
4	*t*Bu	KO*t*Bu (10 mol%)	13
5	Me	KHMDS	0
6	*t*Bu	KHMDS	100
7	Me	KOH	28
8	Me	K_2CO_3	0

Conditions: 0.5 mmol ester, 0.75 mol% of **2**, 20 mol% of KO*t*Bu (except for entry 6), 50 bar H_2 in 1,4-dioxane at 100 °C for 2 h. The yield was determined by GC analysis with *p*-xylene as internal standard.
[a] Yield after 5 h.

Please cite this article in press as: S.N. Sluijter, et al., Journal of Organometallic Chemistry (2017), http://dx.doi.org/10.1016/j.jorganchem.2017.01.003

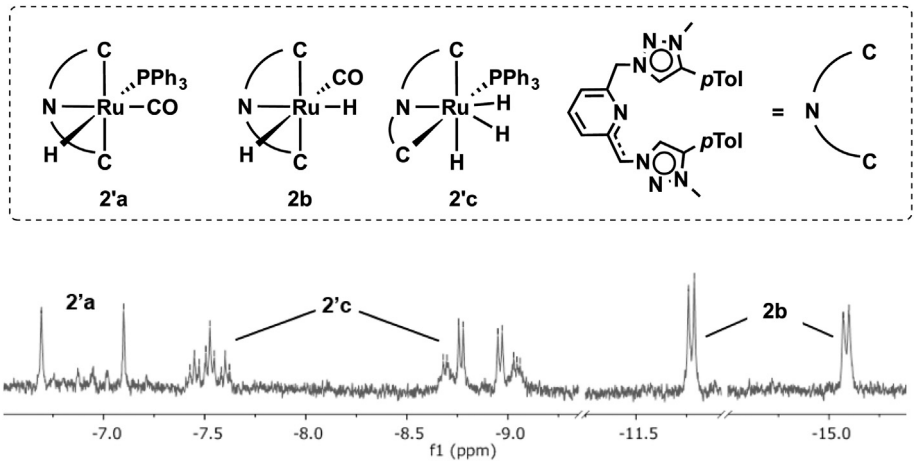

Fig. 1. Postulated structures (top – **2'a** and **2'c** contain a deprotonated monoanionic version of the CNC ligand **L1**; **2b** contains the neutral ligand **L1**) and hydride region of ^{1}H NMR spectrum (bottom) of complexes formed from **2** and KO*t*Bu under 5 bar H_2 after 2 h at 100 °C.

role of the base and iii) substrate transesterification, are discussed here. Like many other ester hydrogenation catalysts, complexes **2** and **5** have a cooperative functionality incorporated in their ligand design that shows the expected reversible deprotonation/dearomatization reactivity upon addition of one equivalent of KO*t*Bu. The proposed active species **2'a** and **2'c** contain a deprotonated ligand, whereas **2b** does not, but this species is possibly in equilibrium with the other two species. It is therefore likely that the triazole-based ligand participates in the catalytic cycle, e.g. in the hydrogen transfer and/or hemiacetal decomposition (Scheme 2). This has also suggested been suggested for a similar *fac*-SNS system [15].

It is remarkable that a minimal amount of KO*t*Bu (≥20 mol%) is necessary to achieve high conversions in the ester hydrogenation with our Ru-systems. Although the requirement for a base or the accelerating effect of a base was previously noted [14,21,32], the exact role of the base in ester hydrogenation has hardly been investigated. For the Co-catalyzed ester hydrogenation of alkyl alkanoate substrates, the basic conditions generate enolate derivatives that are susceptible to hydrogenolysis [35]. However, non-enolizable esters (e.g. methyl benzoate and methyl trifluoracetate) were not converted by this system, which is in contrast with our observations. Thus this mechanism cannot be operative for our system. Alkoxide intermediates of the *trans*-[Ru((*R*)-BINAP)(H)$_2$(*R*,*R*)-dpen)] lactone/ester hydrogenation catalyst were spectroscopically observed by Bergens et al. They argued that the base facilitates elimination of the alkoxide for H_2 on the metal through deprotonation of the bifunctional group in their proposed mechanism.[31,49] Such a mechanism might be plausible for our system, considering the similar *facial* coordination of the ligand around the metal center and the results discussed below.

Our results suggest that the beneficial effect of KO*t*Bu on the ester hydrogenation activity may relate to transesterification of substrates to the corresponding *tert*-butyl ester derivatives [26]. We found that the bulky substrates are hydrogenated considerably faster than methyl esters. This might be explained by *tert*-butoxide being a better leaving group than methoxide. Another explanation may be that methanol has an inhibiting effect by reacting with the deprotonated complex to form a Ru-alkoxide [32]. *tert*-Butanol is likely too bulky to show this undesirable reactivity and additional base has proven to push the equilibrium towards to the formation of the alcohol(s) [27,32]. Lastly, the *tert*-butyl ester might inhibit the inner-sphere mechanism (too bulky) and be transformed via the (faster) outer-sphere mechanism. Overall, the role of the base in the ester hydrogenation mechanism is complex. It participates in deprotonation of the ligand, inducing metal-ligand cooperativity, as well as in transesterification of the substrate, and possibly also in enhancing product expulsion from the catalyst.

3. Conclusions

Novel lutidine-derived CNC and CNN pincer ligands, **L1** and **L2**, have been developed. Coordination of the ligands *via* transmetalation of the corresponding Ag(I) complex led to Ru^{II} complexes **2** and **5**, with rare *facial* coordination of the tridentate ligands. The complexes showed (reversible) deprotonation/dearomatization reactivity upon addition of one equivalent of KO*t*Bu. The Ru^{II} species are active pre-catalysts for the hydrogenolysis of a range of aromatic and aliphatic esters at 100 °C in the presence of 20 mol% KO*t*Bu. Potentially active Ru(CNC)(hydride) species have been detected by NMR spectroscopy under near-catalytic conditions. The mechanistic findings in this work confirm that the catalysis is very complex, with a combination of metal-ligand cooperativity, transesterification, effects of base strength and product inhibition at work.

Acknowledgements

We thank the Dutch National Research School Combination Catalysis Controlled by Chemical Design (NRSC-Catalysis) for financial support within project CJE_2009-13 and Ed Zuidinga and Jan-Meine Ernsting for valuable technical assistance.

Appendix A. Supplementary data

Supplementary data related to this article can be found at http://dx.doi.org/10.1016/j.jorganchem.2017.01.003.

References

[1] (a) D. Morales-Morales, C.M. Jensen, The Chemistry of Pincer Compounds, Elsevier, Amsterdam, 2007;
(b) G. van Koten, D. Milstein, Organometallic Pincer Chemistry, Springer, 2013;
(c) K.J. Szabo, O.F. Wendt, Pincer and Pincer-type Complexes: Applications in Organic Synthesis and Catalysis, Wiley-VCH, 2014;
(d) G. van Koten, R.A. Gossage, The Privileged Pincer-metal Platform: Coordination Chemistry & Applications, Springer, 2017.
[2] (a) S. Musa, I. Shaposhnikov, S. Cohen, D. Gelman, Angew. Chem. Int. Ed. 50 (2011) 3533;

(b) S. Musa, A. Ghosh, L. Vaccaro, L. Ackermann, D. Gelman, Adv. Synth. Catal. 357 (2015) 2351;
(c) S. De-Botton, R. Romm, G. Bensoussan, M. Hitrik, S. Musa, D. Gelman, Dalton Trans. 45 (2016) 16040;
(d) C.M. Moore, N.K. Szymczak, Chem. Commun. 49 (2013) 400;
(e) J.B. Geri, N.K. Szymczak, J. Am. Chem. Soc. 137 (2015) 12808;
(f) C.M. Moore, B. Bark, N.K. Szymczak, ACS Catal. 6 (2016) 1981.

[3] (a) S. Schneider, J. Meiners, B. Askevold, Eur. J. Inorg. Chem. (2012) 412;
(b) B. Zhao, Z. Han, K. Ding, Angew. Chem. Int. Ed. 52 (2013) 4744;
(c) E. Alberico, A.J.J. Lennox, L.K. Vogt, H. Jiao, W. Baumann, H.-J. Drexler, M. Nielsen, A. Spannenberg, M.P. Checinski, H. Junge, M. Beller, J. Am. Chem. Soc. (2016), http://dx.doi.org/10.1021/jacs.6b05692;
(d) M. Nielsen, E. Alberico, W. Baumann, H.-J. Drexler, H. Junge, S. Gladiali, M. Beller, Nature 495 (2013) 85;
(e) M. Nielsen, A. Kammer, D. Cozzula, H. Junge, S. Gladiali, M. Beller, Angew. Chem. Int. Ed. 50 (2011) 9593;
(f) M. Bertoli, A. Choualeb, A.J. Lough, B. Moore, D. Spasyuk, D.G. Gusev, Organometallics 30 (2011) 3479;
(g) S. Chakraborty, P.O. Lagaditis, M. Förster, E.A. Bielinski, N. Hazari, M.C. Holthausen, W.D. Jones, S. Schneider, ACS Catal. 4 (2014) 3994;
(h) P.J. Bonitatibus Jr., S. Chakraborty, M.D. Doherty, O. Siclovana, W.D. Jones, G.L. Soloveichik, Proc. Natl. Acad. Sci. U. S. A. 112 (2015) 1687;
(i) S. Chakraborty, W. W. Brennessel, W. D. Jones, J. Am. Chem. Soc. (136) 8564;. (j) K.T. Tseng, J.W. Kampf, N.K. Szymczak, ACS Catal. 5 (2015) 5468.

[4] (a) S. Oldenhof, B. de Bruin, M. Lutz, M.A. Siegler, F.W. Patureau, J.I. van der Vlugt, J.N.H. Reek, Chem. Eur. J. 19 (2013) 11507;
(b) S. Oldenhof, M. Lutz, B. de Bruin, J.I. van der Vlugt, J.N.H. Reek, Chem. Sci. 6 (2015) 1027;
(c) S. Oldenhof, F.G. Terrade, M. Lutz, J.I. van der Vlugt, J.N.H. Reek, Organometallics 34 (2015) 3209.

[5] (a) K. Umehara, S. Kuwata, T. Ikariya, J. Am. Chem. Soc. 135 (2014) 6754;
(b) S. Kuwata, T. Ikariya, Chem. Commun. 50 (2014) 14290;
(c) T. Toda, S. Kuwata, T. Ikariya, Chem. Eur. J. 20 (2014) 9539;
(d) T. Toda, A. Yoshinari, T. Ikariya, S. Kuwata, Chem. Eur. J. 22 (2016) 16675.

[6] (a) L.S. Jongbloed, B. de Bruin, J.N.H. Reek, M. Lutz, J.I. van der Vlugt, Chem. Eur. J. 21 (2015) 7297;
(b) L.S. Jongbloed, B. de Bruin, J.N.H. Reek, M. Lutz, J.I. van der Vlugt, Catal. Sci. Technol. 6 (2016) 1320;
(c) L.S. Jongbloed, D. García-López, R. van Heck, M.A. Siegler, J.J. Carbó, J.I. van der Vlugt, Inorg. Chem. 55 (2016) 8041;
(d) J. Becker, T. Modl, V.H. Gessner, Chem. Eur. J. 20 (2014) 11295;
(e) J. Weismann, R. Waterman, V.H. Gessner, Chem. Eur. J. 22 (2016) 3846;
(f) L.T. Ghoochany, C. Kerner, S. Farsadpour, F. Menges, Y. Sun, G. Niedner-Schatteburg, W.R. Thiel, Eur. J. Inorg. Chem. (2013) 4305;
(g) K. Ghatak, M. Mane, K. Vanka, ACS Catal. 3 (2013) 920;
(h) C. Boulho, J.-P. Djukic, Dalton Trans. 39 (2010) 8883.

[7] (a) J. Khusnutdinova, D. Milstein, Angew. Chem. Int. Ed. 54 (2015) 12236;
(b) T. Zell, D. Milstein, Acc. Chem. Res. 48 (2015) 1979;
(c) S.Y. de Boer, Y. Gloaguen, J.N.H. Reek, M. Lutz, J.I. van der Vlugt, Dalton Trans. 41 (2012) 11276;
(d) S.Y. de Boer, Y. Gloaguen, M. Lutz, J.I. van der Vlugt, Inorg. Chim. Acta 380 (2012) 336;
(e) J.I. van der Vlugt, J.N.H. Reek, Angew. Chem. Int. Ed. 48 (2009) 8832.

[8] (a) R.D. Rieke, D.S. Thakur, B.D. Roberts, G.T. White, J. Am. Oil Chem. Soc. 74 (1997) 333;
(b) R.D. Rieke, D.S. Thakur, B.D. Roberts, G.T. White, J. Am. Oil Chem. Soc. 74 (1997) 341.

[9] H. Adkins, R. Connor, J. Am. Chem. Soc. 53 (1931) 1091.

[10] (a) R.A. Grey, G.P. Pez, A. Wallo, J. Am. Chem. Soc. 103 (1981) 7536;
(b) U. Matteoli, M. Blanchi, G. Menchi, P. Prediani, F. Piacenti, J. Mol. Catal. 22 (1984) 353;
(c) U. Matteoli, G. Menchi, M. Bianchi, F. Piacenti, J. Mol. Catal. 64 (1991) 257.

[11] (a) H.T. Teunissen, C.J. Elsevier, Chem. Commun. (1997) 667;
(b) H.T. Teunissen, C.J. Elsevier, Chem. Commun. (1998) 1367;
(c) M.C. van Engelen, H.T. Teunissen, J.G. de Vries, C.J. Elsevier, J. Mol. Catal. A Chem. 206 (2003) 185.

[12] Reviews:. (a) J. Pritchard, G.A. Filonenko, R. van Putten, E.J.M. Hensen, E.A. Pidko, Chem. Soc. Rev. 44 (2015) 3808;
(b) S. Werkmeister, K. Junge, M. Beller, Org. Proc. Res. Dev. 18 (2014) 289;
(c) C. Gunanathan, D. Milstein, Chem. Rev. 114 (2014) 12024 (Recent contributions:);
(d) T.J. Korstanje, J.I. van der Vlugt, C.J. Elsevier, B. de Bruin, Science 350 (2015) 298;
(e) T. Zell, Y. Ben-David, D. Milstein, Angew. Chem. Int. Ed. 53 (2014) 4685;
(f) S. Chakraborty, H. Dai, P. Bhattacharya, N.T. Fairweather, M.S. Gibson, J.A. Krause, H. Guan, J. Am. Chem. Soc. 136 (2014) 7869;
(g) S. Werkmeister, K. Junge, B. Wendt, E. Alberico, H. Jiao, W. Baumann, H. Junge, F. Gallou, M. Beller, Angew. Chem. Int. Ed. 53 (2014) 8722.

[13] (a) J. Zhang, G. Leitus, Y. Ben-David, D. Milstein, Angew. Chem. Int. Ed. 45 (2006) 1113;
(b) L.A. Saudan, C.M. Saudan, C. Debieux, P. Wyss, Angew. Chem. Int. Ed. 46 (2007) 7473;
(c) W. Kuriyama, T. Matsumoto, O. Ogata, Y. Ino, K. Aoki, S. Tanaka, K. Ishida, T. Kobayashi, N. Sayo, T. Saito, T. Org, Proc. Res. Dev. 16 (2012) 166;
(d) D. Spasyuk, C. Vicent, D.G. Gusev, J. Am. Chem. Soc. 137 (2015) 3743;
(e) G.A. Filonenko, M.J.B. Aguila, E.N. Schulpen, R. van Putten, J. Wiecko, C. Müller, L. Lefort, E.J.M. Hensen, E.A. Pidko, J. Am. Chem. Soc. 137 (2015) 7620;
(f) D. Kim, L. Le, M.J. Drance, K.H. Jensen, K. Bogdanovski, T.N. Cervarich, M.G. Barnard, N.J. Pudalov, S.M.M. Knapp, A.R. Chianese, Organometallics 35 (2016) 982.

[14] (a) D. Spasyuk, S. Smith, D.G. Gusev, Angew. Chem. Int. Ed. 52 (2013) 2538;
(b) M.L. Clarke, Catal. Sci. Technol. 2 (2012) 2418.

[15] F. Hasanayn, A. Baroudi, Organometallics 32 (2013) 2493.

[16] X. Yang, ACS Catal. 2 (2012) 964.

[17] T. Chen, H. Li, S. Qu, B. Zheng, L. He, Z. Lai, Z.-X. Wang, K.-W. Huang, Organometallics 33 (2014) 4152.

[18] (a) E. Fogler, E. Balaraman, Y. Ben-David, G. Leitus, L.J.W. Shimon, D. Milstein, Organometallics 30 (2011) 3826;
(b) Y. Sun, C. Koehler, R. Tan, V.T. Annibale, D. Song, Chem. Commun. 47 (2011) 8349.

[19] S. Takebayashi, S.H. Bergens, Organometallics 28 (2009) 2349.

[20] G.A. Filonenko, D. Smykowski, B.M. Szyja, G. Li, J. Szczygieł, E.J.M. Hensen, E.A. Pidko, ACS Catal. 5 (2015) 1145.

[21] W.W.N. O, R.H. Morris, ACS Catal. 3 (2013) 32.

[22] For a recent review on 1,2,3-triazolylidenes as ligands, see:. (a) K.F. Donnelly, A. Petronilho, M. Albrecht, Dalton Trans. 49 (2013) 1145;
(b) P. Mathew, A. Neels, M. Albrecht, J. Am, Chem. Soc. 130 (2008) 13534;
(c) T. Nakamura, T. Terashima, K. Ogata, S.-I. Fukuzawa, Org. Lett. 13 (2011) 620;
(d) E.M. Schuster, M. Botoshansky, M. Gandelman, Dalton Trans. 40 (2011) 8764;
(e) E.C. Keske, O.V. Zenkina, R. Wang, C.M. Crudden, Organometallics 31 (2012) 6215;
(f) X. Yan, J. Bouffard, G. Guisado-Barrios, B. Donnadieu, G. Bertrand, Chem. Eur. J. 18 (2012) 14627;
(g) K.F. Donnelly, R. Lalrempuia, H. Müller-Bunz, M. Albrecht, Organometallics 31 (2012) 8414;
(h) L.-A. Schaper, L. Graser, X. Wei, R. Zhong, K. Öfele, A. Pöthig, M. Cokoja, B. Bechlars, W.A. Herrmann, F.E. Kühn, Inorg. Chem. 52 (2013) 6142;
(i) S.N. Sluijter, C.J. Elsevier, Organometallics 33 (2014) 6389;
(j) B. Bagh, A.M. McKinty, A.J. Lough, D.W. Stephan, Dalton Trans. 43 (2014) 12842;
(k) L. Suntrup, S. Hohloch, B. Sarkar, Chem. Eur. J. 22 (2016) 18009;
(l) K. Farrell, H. Müller-Bunz, Martin Albrecht, Dalton Trans. 45 (2016) 15859;
(m) G. Kleinhans, M.M. Hansmann, G. Guisado-Barrios, D.C. Liles, G. Bertrand, D.I. Bezuidenhout, J. Am. Chem. Soc. 138 (2016) 15873.

[23] (a) J.D. Crowley, P.H. Bandeen, Dalton Trans. 39 (2010) 612;
(b) J.D. Crowley, P.H. Bandeen, L.R. Hanton, Polyhedron 29 (2010) 70.

[24] D.G. Brown, N. Sanguantrakun, B. Schulze, U.S. Schubert, C.P. Berlinguette, J. Am. Chem. Soc. 134 (2012) 12354.

[25] (a) M. Hernández-Juárez, M. Vaquero, E. Álvarez, V. Salazar, A. Suárez, Dalton Trans. 42 (2012) 351;
(b) M. Hernández-Juárez, J. López-Serrano, P. Lara, J.P. Morales-Cerón, M. Vaquero, E. Álvarez, V. Salazar, A. Suárez, Chem. Eur. J. 21 (2015) 7540.

[26] (a) J.C. Garrison, W.J. Youngs, Chem. Rev. 105 (2005) 3978;
(b) I.J.B. Lin, C.S. Vasam, Coord. Chem. Rev. 251 (2007) 642.

[27] G.A. Filonenko, E. Cosimi, L. Lefort, M.P. Conley, C. Copéret, M. Lutz, E.J.M. Hensen, E.A. Pidko, ACS Catal. 4 (2014) 2667.

[28] According to DFT calculations the facial coordination mode is thermodynamically less stable than the *mer*-conformation and presumably forms as the kinetic product under the reaction conditions, see Supporting Information.

[29] (a) J.I. van der Vlugt, M.A. Siegler, M. Janssen, D. Vogt, A.L. Spek, Organometallics 28 (2009) 7025;
(b) T. Karthikeyan, S. Sankararaman, Tetrahedron Lett. 50 (2009) 5834;
(c) R.S. Simons, P. Custer, C.A. Tessier, W.J. Youngs, Organometallics 22 (2003) 1979.

[30] M.L. Clarke, G.J. Roff, in: J.G. de Vries, J.C. Elsevier (Eds.), Handbook of Homogeneous Hydrogenation, Wiley-VCH, Weinheim, 2007, p. 413.

[31] F.A. Westerhaus, B. Wendt, A. Dumrath, G. Wienhöfer, K. Junge, M. Beller, ChemSusChem 6 (2013) 1001.

[32] R.J. Hamilton, S.H. Bergens, J. Am. Chem. Soc. 128 (2006) 13700.

[33] Alternatively, the corresponding phenolate complex, which can no longer form a ruthenium dihydride species, could be formed. See for example S. Perdriau, M.-C. Chang, E. Otten, H.J. Heeres, J.G. de Vries, Chem. Eur. J. 20 (2014) 15434.

[34] Alternatively, (partial) conversion of the metal(carbene)(hydride) via reductive C-H elimination might occur, although we have not observed this spectroscopically. For some precedent of protonation of *normal* carbenes in the presence of hydrides, see:. (a) D.S. McGuinness, N. Saendig, B.F. Yates, K.J. Cavell, J. Am. Chem. Soc. 123 (2001) 4029;
(b) C. Gandolfi, M. Heckenroth, A. Neels, G. Laurenczy, M. Albrecht, Organometallics 28 (2009) 5112.

[35] D. Srimani, A. Mukherjee, A.F.G. Goldberg, G. Leitus, Y. Diskin-Posner, L.J.W. Shimon, Y. Ben David, D. Milstein, Angew. Chem. Int. Ed. 54 (2015) 12357.

Please cite this article in press as: S.N. Sluijter, et al., Journal of Organometallic Chemistry (2017), http://dx.doi.org/10.1016/j.jorganchem.2017.01.003